Journal of Applied Polymer Science

Electrochemical Deposition of Poly[*N,N′*-ethylene–bis(salicylideneiminato)-nickel(II)] Nanobelts as Electrode Materials for Supercapacitors

Yakun Zhang,[1] Jianling Li,[1] Xindong Wang,[1] Feng Ye,[2] Jun Yang[2]

[1]State Key Laboratory of Advanced Metallurgy, University of Science and Technology of Beijing, 30 College Road, Beijing 100083, China

[2]State Key Laboratory of Multiphase Complex Systems, Institute of Process Engineering, Chinese Academy of Sciences, Beijing 100190, China

Correspondence to: J. Li (E-mail: lijianling@ustb.edu.cn)

ABSTRACT: *N,N′*-ethylene–bis(salicylideneiminato)]–nickel(II) [Ni(salen)] was synthesized *in situ* onto the surface of multiwalled carbon nanotubes via a one-step potentiostatic electrodeposition as one-dimensional nanobelts. The synthetic process was free of any templates or additives. Potential played a key role in the formation of the poly[*N,N′*-ethylene–bis(salicylideneiminato)]–nickel(II)] {poly[Ni(salen)]} nanobelts, and the electrical conductivities of the poly[Ni(salen)] decreased with increasing deposition time. The capacitance values of poly[Ni(salen)] were 272, 195, and 146 F/g at 0.05 mA/cm^2 for deposition times of 10, 20, and 30 min, respectively. The capacitance of the sample with a particle structure was much lower than that of poly[Ni(salen)] with a nanobelt structure. The poly[Ni(salen)] nanobelts exhibited a better capacitive behavior than the poly[Ni(salen)] particles because the nanobelt structure made access for the charge and ion to the inner part of the electrode easier. © 2013 Wiley Periodicals, Inc. J. Appl. Polym. Sci. **2014**, *131*, 39561.

KEYWORDS: batteries and fuel cells; conducting polymers; electrochemistry; nanostructured polymers

Received 10 January 2013; accepted 19 May 2013

DOI: 10.1002/app.39561

INTRODUCTION

Nanoscale approaches to electrochemical energy storage applications such as supercapacitors have been of great interest with their unique properties, which lead to improved performances.[1–3] The electrode materials significantly influence the properties of supercapacitors, and many scientists have focused on the development of electrode materials with high specific capacitance and good conductivity values.[4–6] Among the explored preparation methods, electropolymerization is a particularly attractive method because of its virtues of cleanliness, safety, efficiency, and low cost,[7,8] and it can be widely used to prepare conducting polymers, metals, and metal oxides.[9] Changes in the synthetic parameters will result in samples with different physical, chemical, and electrochemical properties. Extensive studies have focused on polymer electropolymerization, and the obtained morphologies have included particles, stubs, and film,[8,10,11] which are disadvantageous to ion transfer and diffusion. Hence, great efforts have been made to change the structure through templates or additives,[12] but templates or additives bring about inactive substances or require a further posttreatment process.

The potentiostatic technique[9] was used for the electrodeposition of *N,N′*-ethylene–bis(salicylideneiminato)]–nickel(II) [Ni(salen)], which is a derivative from the archetype of Schiff base metal complexes. This type of transition-metal complex can be anodically polymerized to generate electroactive films in solvents with low donor numbers. The redox switching of electroactive films in a nonaqueous electrolyte system can reversibly achieved in the oxidation/neutral state at high potential[13,14] and the neutral/reduction state at low potential.[15,16] Poly[*N,N′*-ethylene–bis(salicylideneiminato)]–nickel(II)] {poly[Ni(salen)]} was obtained as a nanobelt structure without any templates or additives first. The synthesis conditions determine the intrinsic properties of poly[Ni(salen)]. The effects of the preparation parameters, such as the potential and deposition time, were evaluated by a galvanostatic charge/discharge test. The electrochemical properties of poly[Ni(salen)] were enhanced greatly by the modification of the morphology. This simple one-dimensional nanobelt poly[Ni(salen)] preparation method may create potential for applications in supercapacitors.

EXPERIMENTAL

In a typical experiment procedure, multiwalled carbon nanotubes (MWCNTs) were pretreated by concentrated HNO_3 and H_2SO_4 (volume ratio = 1:3) to get functional groups. Then, the

© 2013 Wiley Periodicals, Inc.

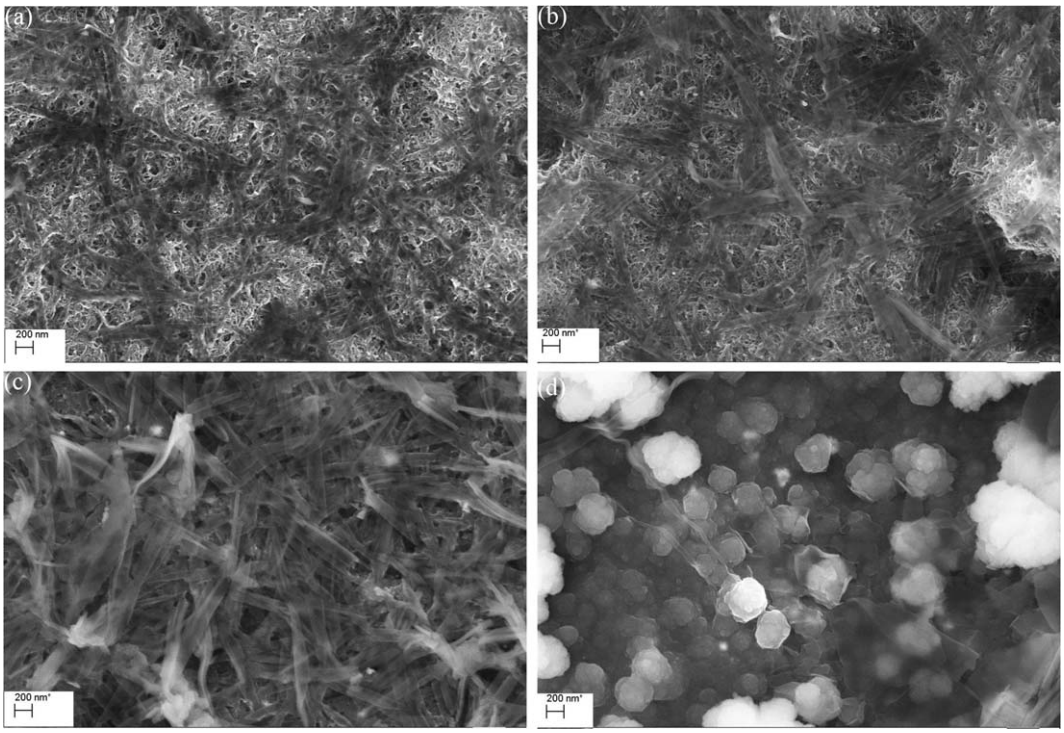

Figure 1. SEM images of poly[Ni(salen)]: (a) PM-1 (0.85 V, 10 min), (b) PM-2 (0.85 V, 20 min), (c) PM-3 (0.85 V, 30 min), and (d) PM-4 (0.95 V, 10 min).

MWCNTs were dispersed in *N*-methyl-2-pyrrolidone by an ultrasonic homogenizer. The slurry was coated on a Ti sheet (current collector, 1 × 1 cm^2) with a coating mass of 0.3 mg. The electrodeposition of Ni(salen) was performed in an acetonitrile solution containing 1.0 mmol/L Ni(salen) monomer and 0.1 mol/L tetrabutyl ammonium perchlorate by potentiostatic electrodeposition at 0.85 V for 10 min. Then, experiments were conducted through the variation of the potential or deposition time.

The morphologies of the obtained materials were characterized by field emission scanning electron microscopy (SEM; Zeiss SuprA 55 microscope, Germany) and transmission electron microscopy (TEM; JEOL JEM 2011). The electrochemical properties were studied by galvanostatic charge/discharge technologies in a VMP2 electrochemical workstation. The electrochemical tests were done in 1.0 mol/L Et_3MeNBF_4 (triethylmethylammonium tetrafluoroborate) in acetonitrile electrolyte with a three-electrode cell composed of a polymer-coated electrode and an Ag/AgCl capillary wire as the auxiliary and reference electrode, respectively, and an activated carbon sheet as a counter.

RESULTS AND DISCUSSION

SEM observation [Figure 1(a)] revealed that the products had remarkable beltlike nanostructures; meanwhile, the amount of poly[Ni(salen)] nanobelts was dominated by the deposition time. The poly[Ni(salen)] nanobelt was about 1–2 μm in length and 100–200 nm wide. Figure 1(c) shows that when the deposition time was increased to 30 min, the amount of nanobelts increased significantly. The amounts of poly[Ni(salen)] are listed in Table I. Obviously, at 0.85 V, along with the increase in the deposition time, the amount of poly[Ni(salen)] increased. Also, at a deposition time of 10 min, the amount of poly[Ni(salen)] at 0.95 V was larger than that at 0.85 V.

As shown in Figure 1(a–c), the poly[Ni(salen)] nanobelts grew more and more with increasing deposition time. To further confirm the formation conditions of the nanobelts, poly[Ni(salen)] was prepared at 0.95 V for 10 min, and the morphology is shown in Figure 1(d). It was clear that the poly[Ni(salen)] deposited at 0.85 V with 10 min [Figure 1(a)] exhibited a nanobelt structure, whereas that deposited at 0.95 V presented a particle structure [Figure 1(d)]. The chain of poly[Ni(salen)] was susceptible to crosslinking action at a higher potential, and this was advantageous for the formation of particles. The impact of the potential on the growth morphology of poly[Ni(salen)] was in accordance with the nucleation and growth mechanism of the polymer via chronoamperometry technology.[17,18]

To further characterize the structure, TEM was used to confirm the beltlike structures, as shown in the SEM images. Figure 2(a) shows the high-resolution TEM microstructure of a carbon nanotube, and we observed that the diameter of the carbon nanotube was about 10–20 nm. The width of the

Table I. Conductivities of the Poly[Ni(salen)] Samples

	PM-1	PM-2	PM-3	PM-4
σ_{ion} (mS/cm)	0.013	0.065	0.049	0.011
σ_e (mS/cm)	0.693	0.100	0.086	0.038
M (mg)	0.0326	0.1134	0.1875	0.0771

σ_{ion} = ionic conductivity; σ_e = electronic conductivity; *M* = the amounts of poly[Ni(salen)].

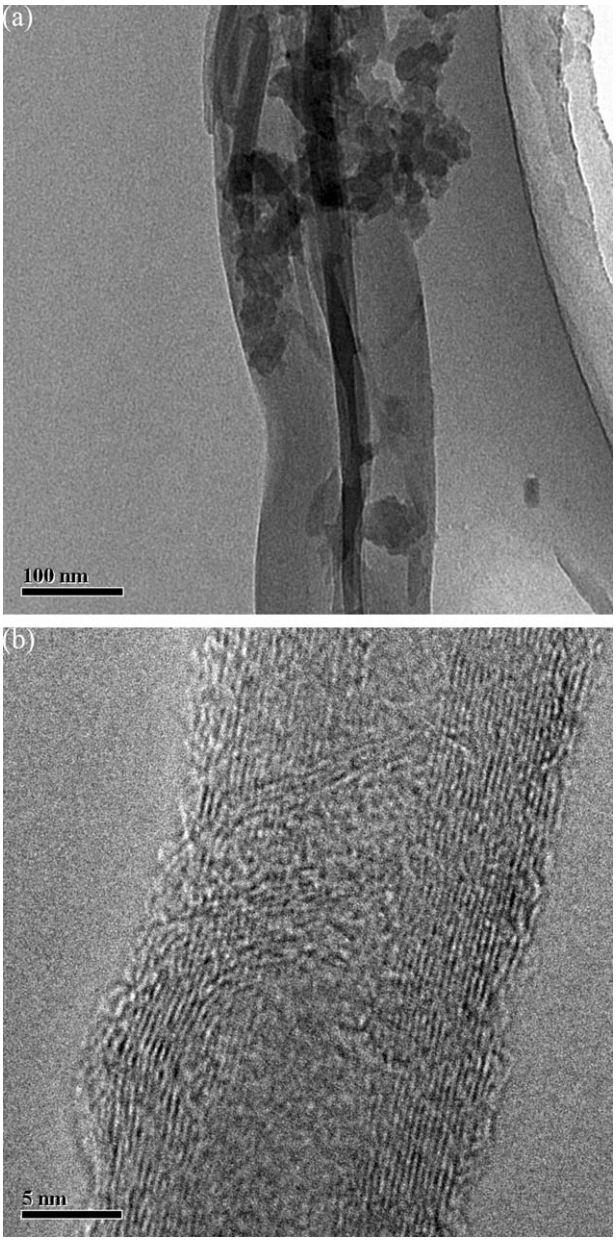

Figure 2. TEM images of the (a) MWCNT and (b) poly[Ni(salen)] nanobelts.

poly[Ni(salen)] nanobelts, estimated from Figure 2(b), was about 150 nm and was consistent with SEM results.

Impedance data of conducting polymers[19,20] have been widely analyzed to obtain information about charge/ion transmission within polymers with the transmission line model. The improved equivalent circuit was based on the improved transmission line model proposed by Pickup et al.;[21] we adopted this model to determine the distributed ionic resistance and electronic resistance within poly[Ni(salen)]. As shown in Table I, The electronic conductivity, which was calculated from the Nyquist curves of the prepared electrodes in Figure 3, decreased with increasing deposition time. When the amount of poly[Ni(salen)] increased, the ionic conductivity of poly[Ni(salen)] first increased and then decreased. This was because too many nanobelts accumulated

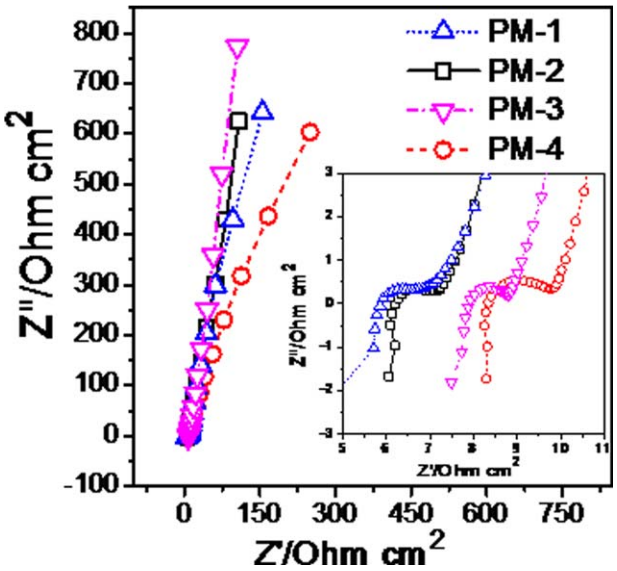

Figure 3. Nyquist curves of the electrodes. Z′ and Z″ represent for the real part and the image part of the impedance respectively. [Color figure can be viewed in the online issue, which is available at wileyonlinelibrary.com.]

and then blocked the spread of ions. Both the electronic conductivity and the ionic conductivity of poly[Ni(salen)] prepared at 0.95 V were poorer than those at 0.85 V. Hence, we concluded that the nanobelt structure was beneficial to the diffusion and transmission of ions and electrons in the electrode.

The typical cyclic voltammograms of the MWCNTs and poly[Ni(salen)]-coated MWCNTs electrodes at different scanning rates are shown in Figure 4. The cyclic voltammetry (CV) plots of the composites possessed a couple of the characteristic redox peaks of poly[Ni(salen)] when the scanning rate increased from 5 to 500 mV/s; this reflected the fact that the poly[Ni(salen)] composites kept a preferable electrochemical activity. From the CV plots, the portion of 0.0–0.4 V at all of the scanning rates showed no obvious change, but the area of responsive currents of the polymer-coated electrode completely covered that of the MWCNTs electrode. This indicated that the polymerization of Ni(salen) on MWCNTs made the double-layer absorption and desorption process on the surface of MWCNTs substrate slightly positive.

Figure 5(a) shows the variation curves of the potential with time. The composites possessed a longer charge/discharge time than the MWCNTs, even at a tenfold current density, because the poly[Ni(salen)] contributed to the pseudo-capacitance caused by the reversible redox switching between neutral and oxidative states on the basis of the electric double-layer capacitance of the MWCNTs. The reversible transition between the neutral state and oxidation state of poly[Ni(salen)] was accompanied by the injection/ejection of counter ions, which corresponded to the $Ni^{2+/3+}$ redox processes. Within the polymer film, the process could be interpreted by the following equation:

$$\text{Poly}\,[\text{Ni}\,(\text{salen}\,)]+n\text{BF}_4{}^- \Longleftrightarrow \text{Poly}\,[\text{Ni}\,(\text{salen}\,)]_{\text{ox}}\,(\text{BF}_4)_{\text{n}}+ne^-$$

The capacitances of poly[Ni(salen)] at different discharge current densities are shown in Figure 5(b). It was clear that the

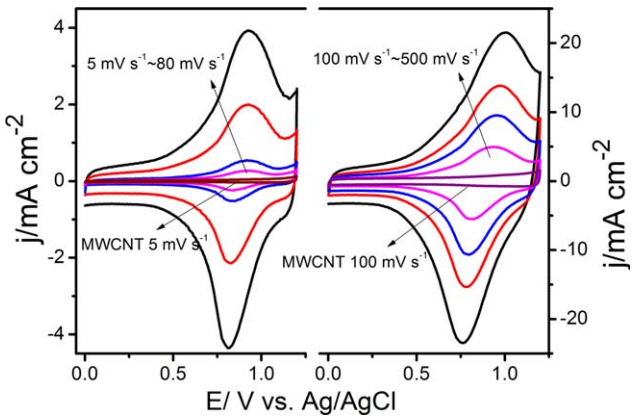

Figure 4. CV plots of the MWCNT and poly[Ni(salen)]-coated MWCNT electrodes at different scan rates. j = current density; E = potential of the poly[Ni(salen)] coated electrode. [Color figure can be viewed in the online issue, which is available at wileyonlinelibrary.com.]

capacitance of poly[Ni(salen)] decreased when the deposition time increased; these were the mixed results of the increasing amount and decreasing conductivity. With increasing current density, the capacitances of all of the samples decreased, and the capacitances declined sharply when the current density was over 8 mA/cm^2. The capacitances of poly[Ni(salen)] were 272, 195, and 146 F/g at 0.05 mA/cm^2 for samples PM-1, PM-2 and PM-3, respectively. The capacitances of sample PM-4 were much lower than those of PM-1; this stemmed from the fact that the structure of the nanobelts made the charge and ion have easier access to the inner part of the electrode, whereas the structure of the agglomeration particles restrained the embedding/emerging of the charge and ion.

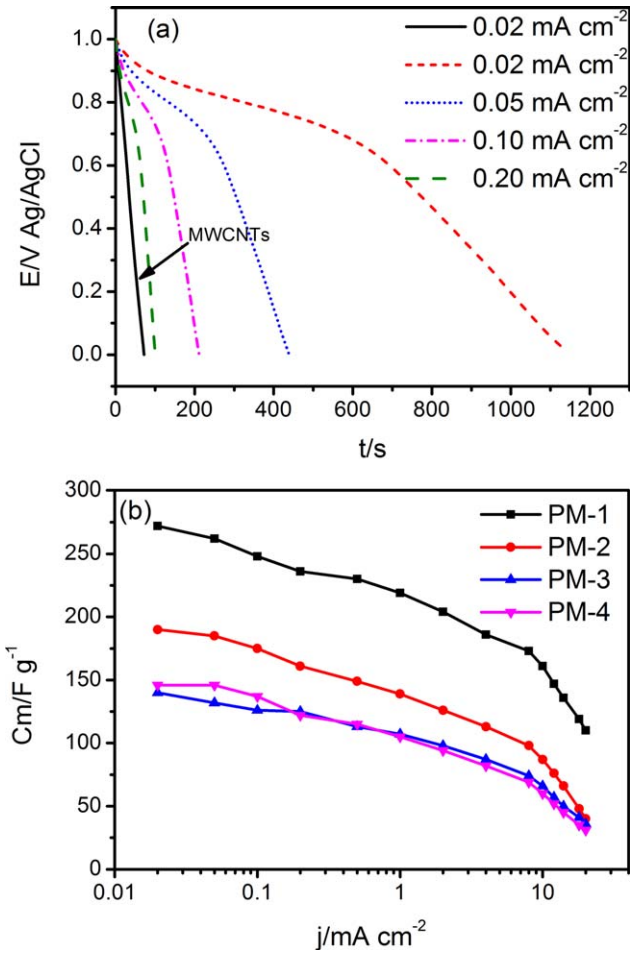

Figure 5. (a) Galvanostatic discharge plots of PM-2 and (b) capacitance–current density relationship. t = discharge time; Cm = capacitance of poly[Ni(salen)]. [Color figure can be viewed in the online issue, which is available at wileyonlinelibrary.com.]

CONCLUSIONS

In summary, poly[Ni(salen)] nanobelts were successfully synthesized via a simple, rapid, and efficient electrochemical approach. The experimental results suggest that the potential played a key role in the formation of the poly[Ni(salen)] nanobelt. The electroconductivity of the poly[Ni(salen)] nanobelts decreased with increasing deposition time. The pseudo-capacitance performance was clearly observed for the prepared electrode, and the specific capacitance of poly[Ni(salen)] could be enhanced by morphological modification. We generally believe that this electrochemical synthetic route could be applied to prepare other electroactive polymer nanobelts.

ACKNOWLEDGMENTS

This work was financially supported by the National Natural Foundation of China (No. 51372021), the Program for New Century Excellent Talents in University (contract grant number NCET-09-0215), the National High Technology Research and Development Program of China (863 Program, contract grant number 2012AA110302), and the State Key Laboratory of Multiphase Complex Systems (contract grant number MPCS-2011-D-08).

REFERENCES

1. Peng, H.; Ma, G.; Ying, W.; Wang, A.; Huang, H.; Lei, Z. *J. Power Sources* **2012**, *211*, 40.
2. Noël, V.; Randriamahazaka, H. N. *Electrochem. Commun.* **2012**, *19*, 32.
3. Yuan, Y. F.; Xia, X. H.; Wu, J. B.; Huang, X. H.; Pei, Y. B.; Yang, J. L.; Guo, S. Y. *Electrochem. Commun.* **2011**, *13*, 1123.
4. McDonough, J. K.; Frolov, A. I.; Presser, V.; Niu, J.; Miller, C. H.; Ubieto, T.; Fedorov, M. V.; Gogotsi, Y. *Carbon* **2012**, *50*, 3298.
5. Chang, H. H.; Chang, C. K.; Tsai, Y. C.; Liao, C. S. *Carbon* **2012**, *50*, 2331.
6. Heli, H.; Yadegari, H.; Jabbari, A. *Mater. Chem. Phys.* **2012**, *134*, 21.
7. Sharma, R. K.; Rastogi, A. C.; Desu, S. B. *Electrochem. Commun.* **2008**, *10*, 268.
8. Li, J. L.; Gao, F.; Kang, F. Y.; Zhang, Y. K.; Wang, X. D.; Ye, F.; Yang, J. *J. Phys. Chem. C* **2011**, *115*, 11822.
9. Kung, C. W.; Chen, H. W.; Lin, C. Y.; Vittal, R.; Ho, K. C. *J. Power Sources* **2012**, *214*, 91.

10. Zou, W. Y.; Wang, W.; He, B. L.; Sun, M.; Yin, Y. *J. Power Sources* **2010**, *195*, 7489.
11. Zhang, B.; Ye, D.; Li, J.; Zhu, X.; Liao, Q. *J. Power Sources* **2012**, *214*, 277.
12. She, M. S.; Ho, R. M. *Polymer* **2012**, *53*, 2628.
13. Hoferkamp, L. A.; Goldsby, K. A. *Chem. Mater.* **1989**, *1*, 348.
14. Audebert, P.; Hapiot, P.; Capdevielle, P.; Maumy, M. *J. Electroanal. Chem.* **1992**, *338*, 269.
15. Dahm, C. E.; Peters, D. G. *Anal. Chem.* **1994**, *66*, 3117.
16. Dahm, C. E.; Peters, D. G.; Simonet, J. *J. Electroanal. Chem.* **1996**, *410*, 163.
17. Chmielewski, M.; Grzeszczuk, M.; Kalenik, J.; Kępas-Suwara, A. *J. Electroanal. Chem.* **2010**, *647*, 169.
18. Raso, M. A.; González-Tejera, M. J.; Carrillo, I.; Sanchez de la Blanca, E.; García, M. V.; Redondo, M. I. *Thin Solid Films* **2011**, *519*, 2387.
19. Shamsipur, M.; Kazemi, S. H.; Mousavi, M. F. *Biosens. Bioelectron.* **2008**, *24*, 104.
20. Uehara, K.; Ichikawa, T.; Matsumoto, K.; Sugimoto, A.; Tsunooka, M.; Inoue, H. *J. Electroanal. Chem.* **1997**, *438*, 85.
21. Ren, X.; Pickup, P. G. *J. Electroanal. Chem.* **1997**, *420*, 251.